Thermal Dissolution of Shengli Lignite in Isometric Methanol and Ethyl Acetate Mixed Solvent — Molecular Composition of the Extract and the Role of Ethyl Acetate

Xingshun Cong[1, a], Min Li[2, b], Hangyu Gao[1, c], Lingling Zhang[1, d], Niancun Ji[1, e]

[1]Department of Chemistry, Zaozhuang University, Zaozhuang, 277160, China

[2]College of Chemical Engineering, China University of Petroleum, Qingdao, 266580, China

[a]email: cxshouse@sohu.com, [b]email: zaoyuanlimin@126.com, [c]email: 18463287480@163.com, [d]email: 18463287173@163.com, [e]email: m17863252269@163.com

Keywords: Shengli Lignite; Phenols; Thermal Dissolution Mechanism; Hydrogen Bond

Abstract. Thermal dissolution (TD) of Shengli lignite was carried out in isometric solvent of methanol and ethyl acetate (EA), methanol, and EA to offer the thermally soluble fractions 1-3 (F_1-F_3), respectively. F_1-F_3 were analyzed by gas chromatography/mass spectrometry and direct analysis in real-time ionization source/ion trap mass spectrometry (DARTIS/IT-MS). Phenols with 1-4 methyls are the most abundant composition in the extract. The DARTIS/IT-MS analysis shows that the main peaks of the molecular weight distribution of the extract are located at *m/z* 120-340, and trace signals are still observed at *m/z* 640. The extract yield of F_1 is higher than those of F_2 and F_3, even the sum of F_2 and F_3 yields. The roles of EA to lignite TD were investigated by experimental comparison and molecular dynamics simulation. Both the increase in nucleophilicity and the O-H bond extension of methanol due to the formation of intermolecular hydrogen bonds between methanol and EA make the nucleophilic attacking and the scission of O-H bond easier. The transesterification reaction with EA occurs during lignite TD. These results demonstrate that the TD process can be slightly adjusted by altering the microstructure and microenvironment of methanol.

Introduction

Understanding of lignite structure, especially macromolecular structure, and then directionally cleaving the specific chemical bonds of lignites to produce clean fuels and value-added chemicals are challenging and attractive tasks. The room-temperature extraction of lignites is a typical method to examine lignite structure [1-3]. However, unlike bituminous coals, the extraction yields of lignites are very small even with isometric carbon disulfide and *N*-methyl-2-pyrrolidinone mixed solvent [4,5] because lignites retain macromolecular species from coal-forming plants. Hence, it is of the utmost importance to enhance the dissolvability of lignites via thermal dissolution (TD) in low-carbon alkanols under relatively mild condition (usually 250-350 ^{o}C, 4-17 MPa). Wei et al [6] investigated alkanolysis of Huolinguole lignite in methanol and in ethanol sequentially at different temperatures and concluded that the nucleophilicity and the solubility parameter of alkanols affected the amount of alkanolysis products. To our knowledge, no reports were issued on TD of any coal in isometric methanol and ethyl acetate (EA) mixed solvent (IMEAMS). The objectives of this research are to analyze molecular components of TD organic matter (TDOM) of Shengli lignite (SL, a Chinese lignite) in IMEAMS and to investigate the TD mechanisms to understand the influence of EA on TD of SL.

Experimental

SL collected form Shengli coal mine, Xilinhaote, Inner Mongolia, China, was pulverized to pass through a 200-mesh sieve (particle size <75 μm), desiccated in a vacuum at 80 ^{o}C for 24 h, and then stored at room temperature in a well-sealed wide-necked bottle to minimize undesirable oxidation. The proximate and ultimate analyses of SL are described elsewhere [7,8]. Methanol, EA, carbon disulfide and acetone in analytically pure grade were distilled with a Büchi R-210 rotary evaporator

prior to use.

About 1 g SL and *ca.* 20 mL IMEAMS were put into a 100 mL stainless-steel, magnetically stirred autoclave. The autoclave was heated to 300 °C and maintained at the temperature for 2 h. Then the autoclave was immediately cooled to room temperature in a water bath and the reaction mixture was exhaustively extracted with IMEAMS to afford IMEAMS soluble fraction (F_1) and extraction residue. TD of *ca.* 1 g SL in 20 mL methanol and in 20 mL EA were also carried out respectively as a comparison to afford methanol soluble fraction (F_2) and EA soluble fraction (F_3).

The gas chromatography/mass spectrometry (GC/MS) analyses of the extracts were performed on a Hewlett-Packard 6890/5973 gas chromatograph/mass spectrometer equipped with a HP-5MS capillary column and a quadrupole mass analyzer (scanned form *m/z* 33 to 550). The molecular weight distribution (MWD) of the extract was determined using an Agilent XCT ion trap multiple-stage mass spectrometer fitted with an IonSense SVP Source direct analysis in real time ionization source (DARTIS). The TD yields of the extracts were calculated according to the formula $Y_F = W_F/W_{SL,daf}$, where W_F and $W_{SL,daf}$ denote weights of the desolventized extracts (solvent-removed F_1, F_2 and F_3) and SL sample on dry and ash free basis, respectively.

Results and discussion

Molecular composition of the extracts: All the extracts (F_1-F_3) were analyzed by GC/MS. The relative contents (RCs) and number of compounds of group components are summarized in Figure 1. In total, 196, 147 and 128 organic compounds were identified in F_1, F_2 and F_3, respectively, and they can be classified into arenes, phenols, alkanes, methyl esters (MEs), ethyl esters (EEs), alkenes, alkoxyarenes (AAs; including methoxyarenes and ethoxyarenes), organonitrogen compounds (ONCs) and other compounds (OCs). Phenols are the most abundant compounds in F_1 and F_2, both accounting for *ca.* 40%, whereas only 21% were detected in F_3. Although RCs of phenols in F_1 and F_2 are similar, considerably more kinds of phenols were detected in F_1 than that in F_2.
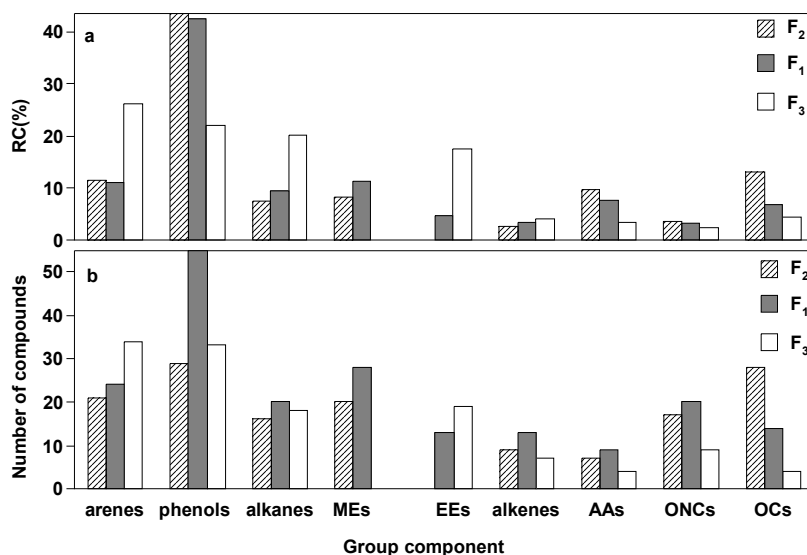

Fig. 1. RCs (a) and number of compounds (b) of group compositions detected in F_1, F_2 and F_3

The total ion chromatogram (TIC) of F_1 is shown in Figure 2. In total, 24 arenes, 55 phenols, 20 alkanes, 28 MAs, 13 EEs, 13 alkenes, 9 AAs, 20 ONCs and 14 OCs were identified. Aliphatic hydrocarbons consist of *n*-alkanes (C_{15}~C_{27}) and *n*-alkenes (C_{14}~C_{23}, without C_{15}, C_{17} and C_{21}), except 5 hopanoids (peaks 185, 187, 189, 191 and 193), 1 cyclopentane (peak 133), 2 cycldienes (peak 7: tetramethylcyclohexadiene and peak 15: dimethylcyclopentadiene) and 2 hexadienes (peaks 18 and 37). Normal fatty acid esters and alkylbenzoic acid esters are the main components in MAs and EEs, accounting for *ca.* 85% and 15%, respectively. All compounds belonged to the arenes, phenols, AAs and OCs are listed in Table 1. Noteworthily, the RC of oxygen-containing compounds in F_1 is 74%, indicating that SL contains substantial amounts of oxygen in the form of carboxyl, phenolic hydroxyl, carbonyl and aromatic ether groups.

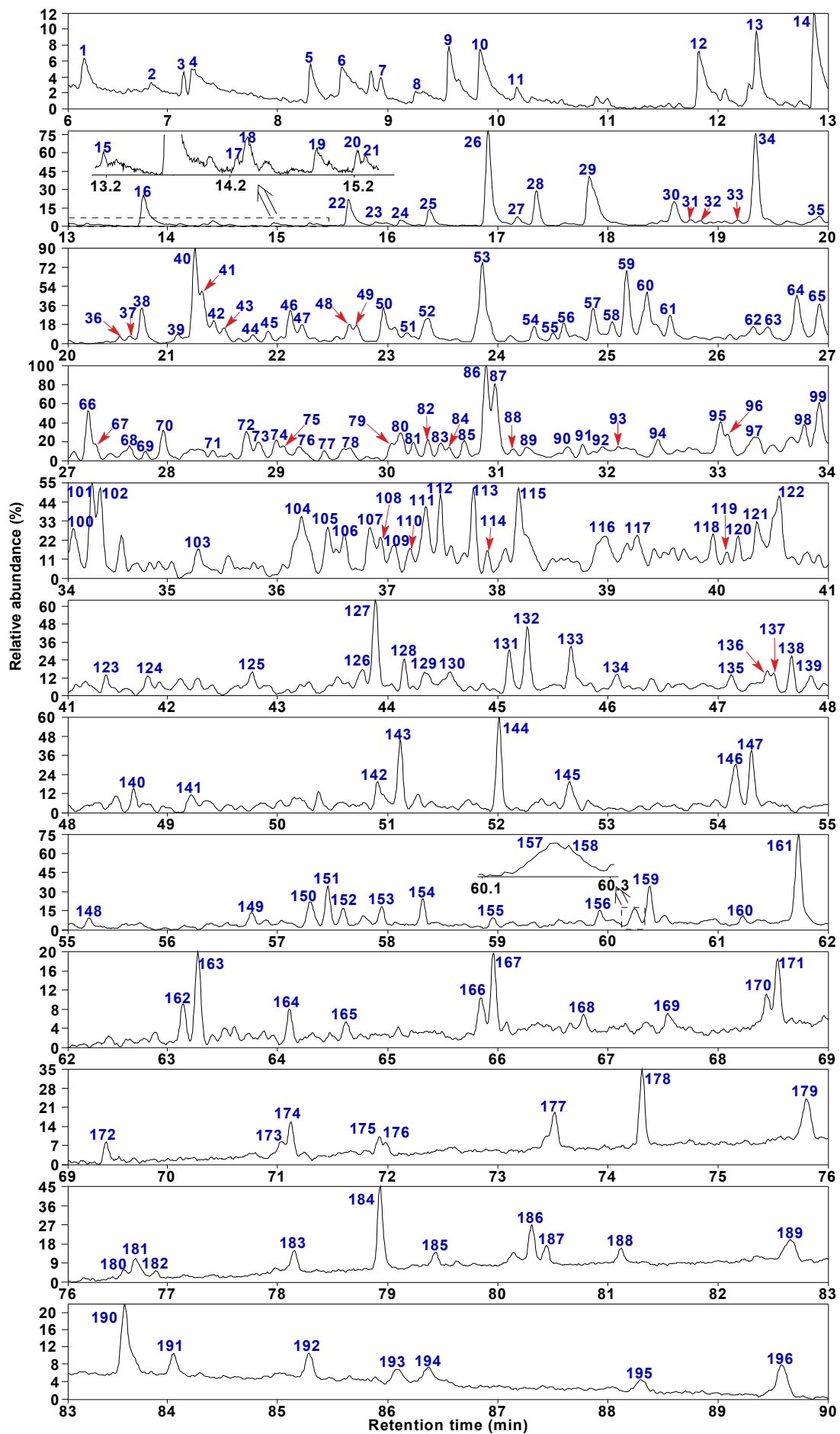Fig. 2. TIC of F$_1$

Table 1. Arenes, phenols, OCs and AAs detected in F_1

Arenes		Phenols		OCs	
Peak	Compounds	Peak	Compounds	Peak	Compounds
3	Toluene	16	Phenol	8	Dimethyl Sulfoxide
90,92	Trimethylindene	26,29	Methylphenol	25	Dimethyl CP
98	Dimethylnaphthalene	34,38,40,41,46-48	C_2-Phenol	27	Methylcyclohex-2-enone
107	Hexamethylbenzene	42,49	Methoxymethylphenol	28,30	Trimethyl CP
114	Dimethylisopropyl THN	43,51	Ethoxyphenol	35,45	Tetramethyl CP
116,122	Trimethylnaphthalene	50,57,61,62	Methylethylphenol	44	HTMCH
127,129	Dimethylisopropylnaphthalene	53,59,64,65,71	Trimethylphenol	80	MTPE
134	Tetramethylnaphthalene	56	Dihydroxy AP	100,101	*Tert*-butylphenylmethanol
135	Tetramethyl THN	58	Isopropylphenol	113	Tetramethyldihydroindenone
139	Anthracene	63	Methoxyethylphenol	125,126	Methylethylbenzothiophene
145	Triisopropylbenzene	66,68,72,74,76-78,81-83,86,87,99	C_4-Phenol		
149	Dimethylphenanthrene	84	Hydroxymethyl AP		AAs
150	Pyrene	85	HMPE	Peak	Compounds
153	Butylhexylnaphthalene	88,96	*Tert*-butylmethylphenol	39	Dimethoxybenzene
155	Fluoranthene	94,103	Methoxytrimethylphenol	52	Methoxyethoxybenzene
156	Trimethylphenanthrene	102	Trimethylbenzenediol	60	Methoxyethylbenzene
161	Methylisopropylphenanthrene	104,106,110,111,118	C_6-Phenol	70	Methoxyisopropylbenzene
165	Dimethylisopropylphenanthrene	108	Neopentyloxyphenol	91	Methoxy-*sec*-butylbenzene
169	Dimethylpyrene	124	Methylnaphthalenol	95,115	MMIB
176	Dinaphthalenylmethane	130	Dimethylnaphthalenol	97	Methoxybutylbenzene
180	Perylene	141	Trimethylnaphthalenol	117	Dimethoxytetramethylbenzene

THN:Tetrahydronaphthalene; C_2: Dimethyl or ethyl; C_6: *Tert*-butyldimethyl, ethylpropyl, or diisopropyl; AP: Acetophenone; C_4: Dimethylethyl, methylisopropyl, diethyl, *sec*-butyl or tetramethyl; HMPE: 1-(2-Hydroxy-5-methoxyphenyl)ethanone; CP: Cyclopent-2-enone; HTMCH: 4-Hydroxy-2,4,5-trimethylcyclohexa-2,5-dienone; MTPE: 1-(4-(Methylthio)phenyl)ethanone; MMIB: Methoxymethylisopropylbenzene.

TD mechanism and the role of EA: As Figure 1(a) exhibits, the RCs (both *ca*. 40%) of phenols in F_1 and F_2 are distinctly higher than that (only 21%) in F_3, which suggested that methanol plays an important role by nucleophilically attacking on C_{acyl} of C_{acyl}-O- moiety and C_{alkyl} of C_{alkyl}-O-C_{aryl} moiety and resulting in the cleavage of oxygen bridges and/or ester bridges during thermal depolymerization. The Y_{F1} is 13.59%, almost equal to the sum of Y_{F2} (10.37%) and Y_{F3} (3.5%), although EA has a lower solubility parameter (18.6 $J^{1/2} \cdot cm^{-3/2}$) than methanol (29.2 $J^{1/2} \cdot cm^{-3/2}$). In addition, distinctly more kinds of phenols were detected in F_1 than that in F_2 as shown in Figure 1(b). These results indicate that the TDOM of 1 g SL in 20 mL IMEAMS is similar in amount with that of 2 g SL in 40 mL separated methanol and EA. These interesting results let us to explore whether there are the cooperative effects and what role EA plays during lignite TD in IMEAMS.

The microstructure and microenvironment of sub- and supercritical methanol are of the utmost importance for the methanolysis reaction during TD of lignite. Yamaguchi et al [9] reported that sub- and supercritical methanol at moderate density exists in hydrogen-bonding oligomers with the average chain-length of *ca*. 3 molecules. Esseffar et al [10] calculated the complexes between methanol and cyclic ketones, lactones, and lactams and showed that the dominant interaction for the most stable complexes is between the oxygen carbonyl and the OH hydrogen of methanol. The theoretical calculations of hydrogen bond between methanol and EA were carried out using the Density Functional Theory. As Figure 3(a) shows, the hydrogen bond between the $O_{carbonyl}$ of EA with the $H_{hydroxyl}$ of methanol (C=O···H-O) is formed, with H···O bond length of 0.1899 nm and O-H···O bond angle of 168°2'. The hydrogen bonding interaction leads to electron transfer from the lone pairs of $O_{carbonyl}$ to the H-O anti-bonding orbital and slightly lengthens the H-O bond by 2×10^{-3} nm, which makes the $O_{hydroxyl}$ of methanol more nucleophilic. As Figure 3(b) exhibits, the $O_{hydroxyl}$ of methanol is the most negative site in the methanol and EA complex. The increase in nucleophilicity of methanol makes the nucleophilic attacking easier at the initial stage of the reaction, and the H-O bond is cleaved readily from the transition state caused by the mentioned H-O bond extension to produce more kinds of phenols as shown in Figure 4. These results demonstrate

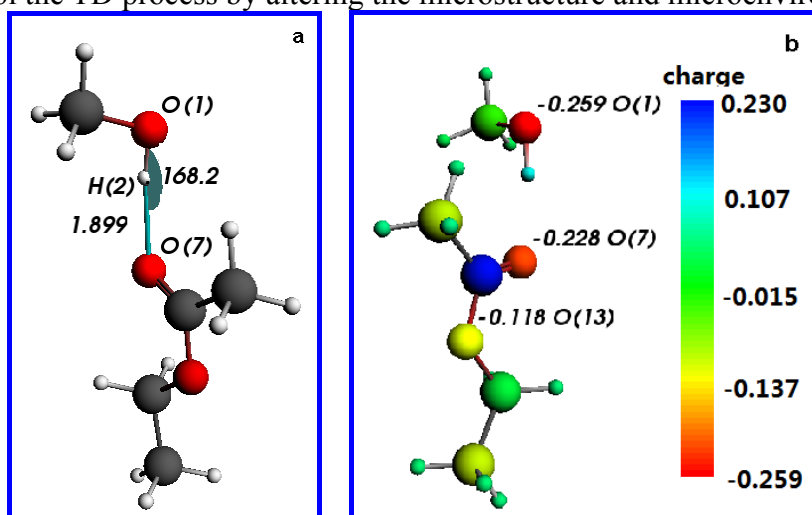that we can control the TD process by altering the microstructure and microenvironment.

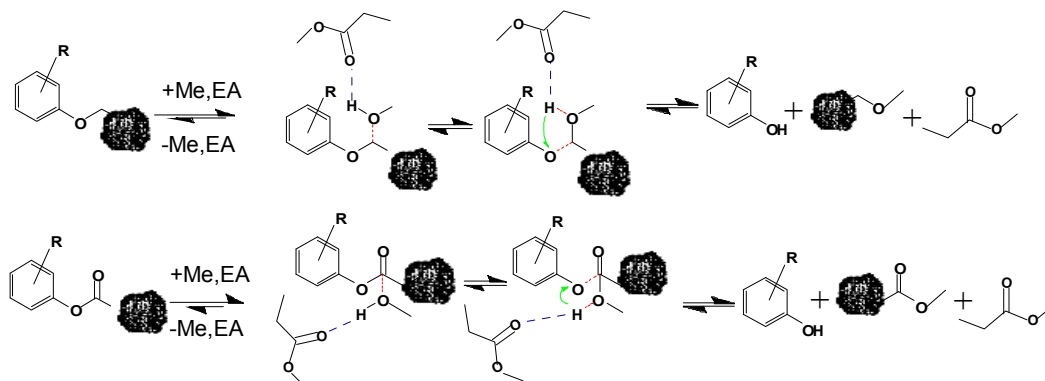Fig. 3. Hydrogen bond (a) and charge distribution (b) of the methanol and EA complex

Fig. 4. Possible phenols formation mechanism during TD of SL in IMEAMS

As Figure 1(a) shows, MEs and EEs were merely detected in F_2 and F_3, respectively, whereas both MEs and EEs appeared in F_1. The RC (17.6%) of EEs in F_3 is substantially higher than that (only 4.6%) in F_2, and slightly more kinds of EEs is detected in F_3 than F_2. These facts indicate that EA possibly involve in the reversible transesterification reaction with esters and carboxylic acids already existing in lignite. EA may react with methanol to produce more nucleophilic ethanol, which in turn undergoes ethanolysis reactions with lignite.

DARTIS/IT-MS analysis of F_1: The MWD measurement of TDOM is fundamental for analyzing and determining their molecular structure. DARTIS permits rapid and direct mass spectrometric detection of gases, liquids, and complex solid samples in open air under ambient conditions. Although the ionization mechanism is still not completely understood, DARTIS mass spectra are relatively simple, dominated by molecular ions and protonated molecules ($[M+H]^+$) in positive ion mode. DARTIS coupled with a mass detector make it especially suitable for the rapid MWD measurement of complex solid samples.
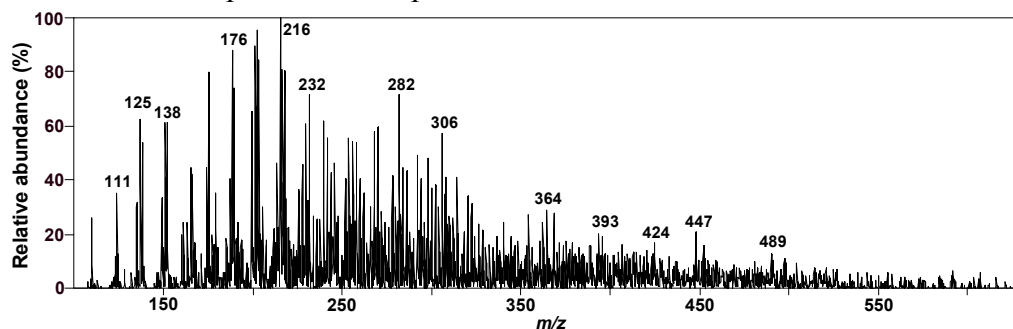

Fig. 5. MWD of F_1 obtained by DARTIS/IT-MS

Figure 5 shows the DARTIS/IT-MS spectra of F_1. The main peaks of the MWD are located at *m/z*

120-340, and trace signals are still observed at m/z 640. Overall, the MWD of F_1 shows a normal distribution, but exhibits clearly incontinuous ion peaks (named cluster-like distribution), especially between m/z 100 and 230. The formation of cluster-like distribution may be due to the structure similarity of the molecules in TDOM, which shows that there are many similar structure units in lignite, and that the isomeric compounds possibly produce via alkylation of lignite with methanol during TD.

Conclusion

IMEAMS proved to be effective for TD of lignite due to the microstructure alterations of methanol and the transesterification reaction of organic species in lignite with EA. Polymethyl phenols are predominant among the 196 organic compounds detected in F_1. The main peaks of the MWD of F_1 are located at m/z 120-340. TD of lignite in IMEAMS is a promising method to examine lignite structure and to convert lignite macromolecules to clean fuels and value-added chemicals.

Acknowledgement

References

[1] X.S. Cong, Z.M. Zong, Z.H. Wei, Y. Li, X. Fan, Y. Zhou, et al. Enrichment and identification of arylhopanes from Shengli lignite. Energy & Fuels 2014, 28:6745-6748.

[2] X.S. Cong, Z.M. Zong, Y. Zhou, M. Li, W.L. Wang, F.G. Li, et al. Isolation and identification of 3-ethyl-8-methyl-2,3-dihydro-1H-cyclopenta[a]chrysene from Shengli lignite. Energy & Fuels 2014, 28:6694-6697.

[3] X.S. Cong, Z.M. Zong, M. Li, L. Gao, Z.H. Wei, Y. Li, et al. Enrichment and identification of cyclized hopanoids from Shengli lignite. Fuel Processing Technology 2015, 134:399-403.

[4] T. Takanohashi, T. Yanagida, M. Iino, D.E. Mainwaring. Extraction and swelling of low-rank coals with various solvents at room temperature. Energy & Fuels 1996, 10:1128-1132.

[5] H. Shui, Z. Wang, J. Gao. Examination of the role of CS_2 in the CS_2/NMP mixed solvents to coal extraction. Fuel Processing Technology 2006, 87:185-190.

[6] H.Y. Lu, X.Y. Wei, R. Yu, Y.L. Peng, X.Z. Qi, L.M. Qie, et al. Sequential thermal dissolution of Huolinguole lignite in methanol and ethanol. Energy & Fuels 2011, 25:2741-2745.

[7] X.S. Cong. Fractional extraction and sequential thermal dissolution of Zhundong subbituminous coal and Shengli lignite. Xuzhou, China University of Mining & Technology, 2014.

[8] X.S. Cong, Z.M. Zong, M. Li, W.L. Wang, X.Y. Wei. Thermal dissolution of Shengli lignite in ethyl acetate: Chemical composition of the extract and mechanism analysis. Journal of Hebei Normal University (Natural Science Edition) 2014, 38:611-616.

[9] T. Yamaguchi, C.J. Benmore, A.K. Soper. The structure of subcritical and supercritical methanol by neutron diffraction, empirical potential structure refinement, and spherical harmonic analysis. The Journal of Chemical Physics 2000, 112:8976-8987.

[10] A. El Firdoussi, M. Esseffar, W. Bouab, J.L.M. Abboud, O. Mó, M. Yáñez, et al. Density functional theory study of the hydrogen bond interaction between lactones, lactams, and methanol. The Journal of Physical Chemistry A 2005, 109:9141-9148.